ISSN 0006-3509, Biophysics, 2022, Vol. 67, No. 5, pp. 734–743. © Pleiades Publishing, Inc., 2022.
Russian Text © The Author(s), 2022, published in Biofizika, 2022, Vol. 67, No. 5, pp. 910–920.

CELL BIOPHYSICS

The Protective Effect of Hydrogen Peroxide on Erythrocyte Hemolysis Induced by Silver Nanoparticles

V. V. Voinarovski[a] and G. G. Martinovich[a,*]

[a] *Belarusian State University, Minsk, 220030 Republic of Belarus*

**e-mail: martinovichgg@bsu.by*

Received April 1, 2021; revised June 3, 2022; accepted June 22, 2022

Abstract—The mechanisms of regulation of adaptation of erythrocytes by hydrogen peroxide during hemolysis induced by silver nanoparticles have been studied using numerical modeling and spectrophotometric analysis. It was shown that silver nanoparticles induced erythrocyte hemolysis, the rate of which depended on the total concentration of silver and the ion content in the solution. Hemolysis of erythrocytes with silver nitrate proceeded twice as fast as with nanoparticles. It was found that hydrogen peroxide increased the structural stability of erythrocytes during hemolysis induced by silver nanoparticles and silver nitrate. The range of hydrogen peroxide concentrations at which an increase in the proportion of non-hemolysed cells (the hormesis region) was observed depended on the time of cell destruction under the action of a damaging factor. The maximum of hormesis was observed at a concentration of hydrogen peroxide of 1250 μM under damage induced by silver nanoparticles; it was 700 μM under damage induced by silver nitrate. Numerical modeling has shown that the dependence of the maximum of hormesis on the concentration of extracellular hydrogen peroxide and incubation time was due to the dynamic nature of cytoplasmic mechanisms regulating the ratio of membrane complexes of methemoglobin and ferryl hemoglobin.

Keywords: hormesis, adaptation, hydrogen peroxide, erythrocytes, methemoglobin, silver nanoparticles

DOI: 10.1134/S0006350922050220

INTRODUCTION

The ability to adapt to stress is the most important characteristic of a healthy body [1]. However, the protective and adaptive mechanisms at the cell level have not been sufficiently studied. The key participants in the regulation of the cell response to stress factors are reactive oxygen species (ROS), highly reactive oxygen metabolism products with a wide range of physiological and pathophysiological effects [2]. ROS include various chemical compounds such as singlet oxygen ($^1O_2$), superoxide ($O_2^{\bullet-}$) and hydroxyl ($HO^{\bullet}$) radicals, hydrogen peroxide (H_2O_2) and others. Hydrogen peroxide is the main molecule of the ROS group that transmits regulatory signals [3]. The signals transmitted by hydrogen peroxide are characterized by their activation concentration threshold and duration. The effect of such signals is reversible and regulated by a multicomponent antioxidant system as a result of the conjugated functioning of specialized proteins such as catalase (Cat), glutathione peroxidase (Gpx), peroxyredoxin (Prx), and others [2].

It has been found that the regulation of gene expression of the antioxidant system proteins in mammalian cells is carried out by the transcription factor Nrf2 (nuclear E2-related factor 2), whose activity is controlled with the participation of the redox-dependent protein Keap1 (Kelch-like ECH-associating protein 1) [4]. The Keap1-Nrf2 system plays a key role in maintaining cellular redox homeostasis under stress and is considered as a potential target for therapy of a wide range of diseases [5, 6]. However, in erythrocytes, the most numerous human blood cells, this system of maintaining redox homeostasis is absent; the protection of cells under stress is carried out by cytoplasmic mechanisms, including the regulation of the functional state of proteins and their interactions with the cell membrane and cytoskeleton.

Increasing the structural stability of the membrane when its components bind to hemoglobin, the main protein of erythrocytes, is the most important mechanism for protecting erythrocytes [7]. The rate constants of the formation and decay of hemoglobin membrane complexes depend on the oxidized state of the protein [8, 9]. The interaction of methemoglobin with membrane components is characterized by a

Abbreviations: ROS, reactive oxygen species; Cat, catalase; Gpx, glutathione peroxidase; Prx, peroxiredoxin; NADH, nicotinamide adenine dinucleotide (reduced form); NAD^+, nicotinamide adenine dinucleotide (oxidized form); NADPH, nicotinamide adenine dinucleotide phosphate (reduced form); $NADP^+$, nicotinamide adenine dinucleotide phosphate (oxidized form); B3, band 3 protein; MetHb, methemoglobin; FerHb, ferrylhemoglobin.

higher binding constant than the binding of oxyhemoglobin. Reversible binding of methemoglobin to cytoskeleton proteins has been shown to have a stabilizing effect on erythrocyte membranes [10, 11]. Reduction of methemoglobin by nicotinamide adenine dinucleotide (NADH), catalyzed by cytochrome b5, leads to a decrease in the number of protein membrane complexes [12]. The accumulation of a more oxidized form of hemoglobin, ferryl hemoglobin, enhances the processes of lipid peroxidation and reduces the structural stability of membranes [13]. The mechanisms of changing the balance of oxidized forms of hemoglobin and their binding to the membrane under the action of external stress factors have not yet been studied.

We have previously shown that the ratio of membrane complexes of various oxidized forms of hemoglobin determined the hormesis dependence of the response of erythrocytes to the action of hydrogen peroxide; namely, it was regulatory at low concentrations and damaging at high concentrations [14]. The range of hydrogen peroxide concentrations at which an increase in the structural stability of the membrane (the hormesis region) was observed depended on a number of internal and external factors.

The significant increase in the production of new materials containing nanoscale particles and the expansion of their application areas has actualized the study of the mechanisms of interaction between artificial nanomaterials and biological systems. Silver nanoparticles are widely used as bactericidal, antiviral, antifungal and antiseptic agents; however, they may exhibit toxic properties in relation to mammalian and human cells [15]. Since the concentration of hydrogen peroxide can change under the action of silver nanoparticles, the conditions and mechanisms of the protective action of the oxidant in cases of damage to erythrocytes induced by silver nanoparticles were studied in this work.

The destruction of cells under the action of silver nanoparticles is mainly caused by silver ions released by nanoparticles [16, 17] and depends on a number of factors, including extracellular and intracellular redox conditions [18]. To quantify the influence of various factors on the action of hydrogen peroxide in erythrocytes, a mathematical model has been constructed in which the transmission of a signal involving hydrogen peroxide and the formation of membrane complexes of oxidized proteins was considered as a chain of interrelated events.

DESCRIPTION OF THE MODEL

The increase in the structural stability of erythrocyte membranes induced by hydrogen peroxide enhances the protective properties of cells and, consequently, reduces the number of cells destroyed during hemolysis. When modeling the hemolysis of erythrocytes induced by nanoparticles, it is assumed that the rate of cell destruction is proportional to the number of cells in the suspension and the amount of silver ions released by nanoparticles that cause destruction. The rate of release of silver ions, in turn, is directly proportional to the number of ions enclosed in nanoparticles and depends on the protective properties of cells. In this case, the rate of change in the number of cells in the suspension is regulated by two competing processes (protection and destruction) and can be described by the following system of equations:

$$\begin{cases} \dfrac{dn}{dt} = -k_d \cdot n \cdot [Ag^+] \\ \dfrac{d[Ag^+]}{dt} = \dfrac{1}{k_p} \cdot [Ag^0] \\ \dfrac{d[Ag^0]}{dt} = -\dfrac{1}{k_p} \cdot [Ag^0], \end{cases} \quad (1)$$

where n is the number of cells in the suspension, k_d is the destruction coefficient, k_p is the protection coefficient, $[Ag^+]$ is the concentration of released silver ions in solution, and $[Ag^0]$ is the concentration of silver ions in the form of nanoparticles. The total concentration of silver is considered constant.

Equation (2) is the solution of the system (1)

$$n(t) = n(0) \times \exp\left([Ag^0](0) k_d \left(k_p - k_p \exp\left(-\frac{t}{k_p} \right) - t \right) \right), \quad (2)$$

where $n(0)$ is the initial number of cells in the suspension, $[Ag^0](0)$ is the initial concentration of silver ions that was used in the synthesis of nanoparticles, and t is the time. The values of coefficients k_d and k_p were determined based on experimentally obtained dependences of erythrocyte hemolysis using the least squares method.

The protective properties of cells during hemolysis are determined by the structural stability of the membrane and are characterized by the protection coefficient k_p. Based on previous studies [14], the model assumed that the structural stability of the membrane depended on the number of membrane complexes of methemoglobin and ferryl hemoglobin and changes over time.

To quantify the dynamics of changes in the protective properties of the cell, the key stages of the formation of methemoglobin and ferrylhemoglobin and their binding to the membrane under the action of extracellular hydrogen peroxide were considered based on the mathematical model described earlier [14]. To consider the influence of silver nanoparticles, a number of changes have been made to the model.

The new model introduces a simplification of the complete system of glycolysis and the pentose phosphate pathway, based on the condition of the steady state of the flows [19]. When determining the rate of

reduction of NADPH and NADH, the rate of glucose transport through the GLUT1 membrane transporter (membrane glucose transporter 1) was considered. It is believed that when one glucose molecule is oxidized, two NAD^+ molecules or two $NADP^+$ molecules are reduced. A decrease in the supply of the energy source (glucose) leads to depletion of the NADPH and NADH pool and changes the rate of glycolysis or the pentose phosphate pathway in proportion to the concentration of pyridine nucleotides. Thus, the new model did not consider the general rates of glycolysis or the pentose phosphate pathway, it considered only deviations from the initial values.

The formation of methemoglobin and ferryl hemoglobin induced by hydrogen peroxide leads to their binding to the components of the erythrocyte membrane. The dynamics of the formation of membrane complexes of oxidized forms of hemoglobin is described by the kinetics of ligand-receptor interaction, where oxidized hemoglobin acts as a ligand, and the membrane Band 3 protein (B3) serves as a receptor. The equilibrium of the processes of binding and dissociation of complexes on the membrane occurs much faster than the processes of reduction of oxidized proteins; therefore, the stationary state of the complexes formed was considered in the model. The number of membrane complexes of methemoglobin and ferryl hemoglobin depends on the content of methemoglobin and ferryl hemoglobin, respectively, in the cytoplasm:

$$\begin{gathered}\mathrm{MetHb} + \mathrm{B3} \underset{k_{-1}}{\overset{k_1}{\rightleftarrows}} \mathrm{MetHb{-}B3},\\ \mathrm{FerHb} + \mathrm{B3} \underset{k_{-2}}{\overset{k_2}{\rightleftarrows}} \mathrm{FerHb{-}B3},\\ [\mathrm{MetHb{-}B3}](t) = \frac{[\mathrm{B3}_0]\cdot k_\mathrm{d}^\mathrm{f}\cdot[\mathrm{MetHb}](t)}{[\mathrm{FerHb}](t)\cdot k_\mathrm{d}^\mathrm{m} + k_\mathrm{d}^\mathrm{m}\cdot k_\mathrm{d}^\mathrm{f} + k_\mathrm{d}^\mathrm{f}\cdot[\mathrm{MetHb}](t)},\\ [\mathrm{FerHb{-}B3}](t) = \frac{[\mathrm{B3}_0]\cdot k_\mathrm{d}^\mathrm{m}\cdot[\mathrm{FerHb}](t)}{[\mathrm{FerHb}](t)\cdot k_\mathrm{d}^\mathrm{m} + k_\mathrm{d}^\mathrm{m}\cdot k_\mathrm{d}^\mathrm{f} + k_\mathrm{d}^\mathrm{f}\cdot[\mathrm{MetHb}](t)}.\end{gathered} \tag{3}$$

where [B3] is the concentration of band 3 proteins available for binding, $[B3_0]$ is the total concentration of band 3 proteins, [MetHb] is the concentration of methemoglobin in the cell, [MetHb–B3] is the concentration of methemoglobin membrane complexes, [FerHb] is the concentration of ferryl hemoglobin in the cell, [FerHb–B3] is the concentration of membrane complexes of ferryl hemoglobin, k_d^f is the dissociation constant of ferryl hemoglobin complexes, and k_d^m is the dissociation constant of methemoglobin complexes.

The constructed mathematical model was nonlinear and contained 17 differential equations. Tables 1 and 2 show these equations and their constants. All constants and initial conditions were taken from the literature. An analysis of the stability of the system was performed.

The numerical solution of the system was performed in the Wolfram Mathematica program. The effect of hydrogen peroxide on the dynamics of changes in the membrane-bound state of oxidized forms of hemoglobin under the action of various damaging factors was studied on the basis of numerical modeling.

MATERIALS AND METHODS

Silver nitrate (LenReactive, Russia) and hydrogen peroxide (Belmedpreparaty, Belarus) were used in the experiments. The blood of healthy donors was received at the State Institution "Republican Scientific and Practical Center of Transfusiology and Medical Biotechnologies" (Minsk, Belarus). The leukocyte layer and blood plasma were separated after double centrifugation at 1500 rpm. Spectrophotometric studies of erythrocytes were carried out in a phosphate-salt buffer containing 10 mM Na_2HPO_4/KH_2PO_4, 137 mM NaCl, 2.7 mM KCl, 5 mM D-glucose (pH 7.4).

Nanoparticles were obtained using the methods of "green chemistry" [18]. A solution of silver nitrate at a concentration of 1 mM was mixed with an aqueous plant extract in a ratio of 9 : 1 at pH 8.0 and incubated for 1 h at room temperature. The end of synthesis was recorded by the appearance of a peak at 400 nm caused by surface plasmon resonance. Nanoparticle sizes were determined by the spectrophotometric method [26]. The quantitative changes of nanoparticles in experiments were expressed in terms of the concentration of silver ions ($[Ag^0]$) necessary for their synthesis.

Hemolysis was initiated by adding silver nanoparticles or silver nitrate to a suspension of erythrocytes. The kinetics of erythrocyte hemolysis was measured by recording the optical density of the cell suspension (30 million of cells/mL) at 680 nm at 37°C. At the end of hemolysis (after 50 min for nanoparticles and 20 min for silver nitrate), the absorption spectra of hemolysate were recorded. The change in the number of cells was assessed by the change in the optical density of the erythrocyte suspension at 680 nm. Osmotic

Table 1. Reactions and rate equations in the model

No.	Reaction and rate equation	The value of constants	References
1	H_2O_2 (external) $\rightarrow H_2O_2$ $v_1 = -P \cdot ([H_2O_2] - [H_2O_2(\text{external})] \cdot \frac{S_{\text{cell}}}{V} \cdot N_{\text{cell}}$	$P = 6 \times 10^{-6}$ m s^{-1} $S_{\text{cell}} = 1.09 \times 10^{-10}$ m^2 $V = 10^{-6}$ m^3 $N_{\text{cell}} = 3 \times 10^7$	[20]
2	H_2O_2 (external) $\rightarrow H_2O_2$ $v_2 = -P \cdot ([H_2O_2] - [H_2O_2(\text{external})] \cdot \frac{S_{\text{cell}}}{V}$	$P = 6 \times 10^{-6}$ m s^{-1} $S_{\text{cell}} = 1.09 \times 10^{-10}$ m^2 $V_{\text{cell}} = 6.3 \times 10^{-17}$ m^3	[20]
3	$H_2O_2 + \text{Cat} \rightarrow H_2O + \text{CompI}$ $v_3 = k_3 \cdot [\text{Cat}] \cdot [H_2O_2]$	$k_3 = 6 \times 10^6$ M^{-1} s^{-1}	[21]
4	$H_2O_2 + \text{CompI} \rightarrow H_2O + O_2 + \text{Cat}$ $v_4 = k_4 \cdot [\text{CompI}] \cdot [H_2O_2]$	$k_4 = 1.6 \times 10^7$ M^{-1}·s^{-1}	[21]
5	$H_2O_2 + 2\text{GSH} \xrightarrow{\text{Gpx}} 2H_2O + \text{GSSG}$ $v_5 = \frac{[\text{Gpx}] \cdot [\text{GSH}] \cdot [H_2O_2]}{K_1 \cdot [H_2O_2] + K_2 \cdot [\text{GSH}]}$	[Gpx] $= 1.4 \times 10^{-6}$ M $K_1 = 2.5 \times 10^{-5}$ M s $K_2 = 2.4 \times 10^{-8}$ M s	[22]
6	$2\text{Hb} + H_2O_2 \rightarrow 2\text{MetHb} + H_2O$ $v_6 = k_6 \cdot [\text{Hb}] \cdot [H_2O_2]$	$k_6 = 100$ M^{-1} s^{-1}	[21]
7	$\text{MetHb} + H_2O_2 \rightarrow \text{FerHb} + H_2O$ $v_7 = k_7 \cdot [\text{MetHb}] \cdot [H_2O_2]$	$k_7 = 98$ M^{-1} s^{-1}	[23]
8	$\text{MetHb} + \text{cytb5(red)} \rightarrow \text{Hb} + \text{cytb5(ox)}$ $v_8 = k_8 \cdot [\text{MetHb}] \cdot [\text{cytb5(red)}]$	$k_8 = 6200$ M^{-1} s^{-1}	[24]
9	$\text{NADH} + \text{cytb5(ox)} \xrightarrow{\text{cytb5R}} \text{NAD}^+ + \text{cytb5(red)}$ $v_9 = \frac{k_9 \cdot [\text{cytb5R}] \cdot [\text{NADH}] \cdot [\text{cytb5(ox)}]}{(K_M^{\text{NADH}} + [\text{NADH}]) \cdot (K_{\text{M}}^{\text{cytb5(ox)}} + [\text{cytb5(ox)}])}$	$k_9 = 418$ s^{-1} [cytb5R] $= 7 \times 10^{-8}$ M $K_{\text{M}}^{\text{NADH}} = 3.1 \times 10^{-7}$ M $K_{\text{M}}^{\text{cyt b5(ox)}} = 1.5 \times 10^{-5}$ M	[24]
10	$\text{FerHb} + 2\text{Asc} \rightarrow \text{MetHb} + \text{DHA} + \text{Asc}$ $v_{10} = k_{10} \cdot [\text{FerHb}] \cdot [\text{Asc}]$	$k_{10} = 400$ M^{-1} s^{-1}	[23]
11	$\text{DHA} + 2\text{GSH} \xrightarrow{\text{DHAR}} \text{Asc} + \text{GSSG}$ $v_{11} = \frac{k_{11} \cdot [\text{DHAR}] \cdot [\text{DHA}] \cdot [\text{GSH}]}{[\text{DHA}] \cdot [\text{GSH}] + K_{\text{DHA}} \cdot [\text{GSH}] + K_{\text{GSH}}[\text{DHA}]}$	$k_{11} = 5.27$ s^{-1} [DHAR] $= 10^{-7}$ M $K_{\text{DHA}} = 2.1 \times 10^{-4}$ M $K_{\text{GSH}} = 3.5 \times 10^{-3}$ M	[25]
12	$\text{GSSG} + \text{NADPH} \xrightarrow{\text{GR}} \text{NADP} + 2\text{GSH}$ $v_{12} = \frac{[\text{GR}] \cdot [\text{GSSG}] \cdot [\text{NADPH}]}{K_1 \cdot [\text{NADPH}] + K_2 \cdot [\text{GSH}]}$	[GR] $= 1.4 \times 10^{-6}$ M $K_1 = 2.4 \times 10^{-8}$ M s $K_2 = 2.5 \times 10^{-5}$ M s	[22]
13	$\text{NAD(P)}^+ \xrightarrow{\text{GLUT1}} \text{NAD(P)H}$ $v_{\text{GLUT}} = \frac{V_{\max} \cdot ([\text{NAD}^+] + [\text{NADP}^+])}{2 \cdot \left(1 + \frac{[\text{glc(external)}]}{K_{\text{ex}}^{\text{m}}} + \frac{[\text{glc(external)}] - 2 \cdot ([\text{NAD}^+] + [\text{NADP}^+])}{K_{\text{in}}^{\text{m}}} + \alpha \cdot \frac{[\text{glc(external)}] \cdot ([\text{glc(external)}] - 2 \cdot ([\text{NAD}^+] + [\text{NADP}^+]))}{K_{\text{ex}}^{\text{m}} \cdot K_{\text{in}}^{\text{m}}}\right)}$	$V_{\max} = 0.0207$ M s^{-1} $K_{\text{ex}}^{\text{m}} = 1.7 \times 10^{-3}$ M $K_{\text{in}}^{\text{m}} = 6.9 \times 10^{-3}$ M $\alpha = 0.54$	[19]

Table 2. The ultimate system of equations in the model

System of equations	Initial values, M
$[Cat]'(t) = -v_3 + v_4$	$[Cat](0) = 5.5 \times 10^{-6}$
$[CompI]'(t) = v_3 - v_4$	$[CompI](0) = 5.5 \times 10^{-6}$
$[H_2O_2(external)]'(t) = -v_1$	$[H_2O_2(external)](0) = (1...1.25) \times 10^{-3}$
$[H_2O_2]'(t) = v_2 - v_3 - v_4 - v_5 - v_6 - v_7$	$[H_2O_2](0) = 0$
$[cytb5(red)]'(t) = -v_8 + v_9$	$[cytb5(red)](0) = 8.1 \times 10^{-6}$
$[cytb5(ox)]'(t) = v_8 - v_9$	$[cytb5(ox)](0) = 0$
$[MetHb]'(t) = v_6 - v_7 - v_8 + v_{10}$	$[MetHb](0) = 0$
$[FerHb]'(t) = v_7 - v_{10}$	$[FerHb](0) = 0$
$[Hb]'(t) = -v_6 + v_8$	$[Hb](0) = 0.01$
$[Asc]'(t) = -v_{10} + v_{11}$	$[Asc](0) = 7.5 \times 10^{-5}$
$[DHA]'(t) = v_{10} - v_{11}$	$[DHA](0) = 0$
$[GSH]'(t) = 2(-v_5 - v_{11} + v_{12})$	$[GSH](0) = 1.5 \times 10^{-3}$
$[GSSG]'(t) = v_5 + v_{11} - v_{12}$	$[GSSG](0) = 0$
$[NADP]'(t) = -v_{GLUT} + v_{12}$	$[NADP](0) = 0.2 \times 10^{-6}$
$[NADPH]'(t) = v_{GLUT} - v_{12}$	$[NADPH](0) = 5 \times 10^{-5}$
$[NAD]'(t) = -v_{GLUT} + v_9$	$[NAD](0) = 8.9 \times 10^{-5}$
$[NADH]'(t) = v_{GLUT} - v_9$	$[NADH](0) = 1.5 \times 10^{-7}$

hemolysis was performed by incubating erythrocytes in solutions with different concentrations of NaCl (48–85 mM).

To determine the protective effect, the cells were incubated with hydrogen peroxide for 10 min before the introduction of a hemolytic factor. The protective effect was determined as an increased proportion of non-hemolysed erythrocytes (N/N_0, where N_0 is the initial number of erythrocytes in suspension, and N is the number of cells after hemolysis) in the presence of an oxidant.

The oxidized form of hemoglobin on the erythrocyte membrane was determined spectrophotometrically after 10 min of incubation with hydrogen peroxide at a concentration of 250 μM after osmotic destruction of the cells. Hemolysis products were isolated by centrifugation for 30 min at 7000 rpm. The absorption spectrum of hemolysate was recorded at 400–450 nm. The measurements were carried out using a CM-2203 spectrofluorimeter and a UV-VIS RV 2201 spectrophotometer (Solar, Republic of Belarus).

The results were presented as averages ± standard deviation of the mean for three to five independent experiments. Statistical analysis was carried out using the Microsoft Excel program. The reliability of the values was determined using the student's t-test, taking the differences as significant at a significance level of $p < 0.05$.

RESULTS AND DISCUSSION

The optical properties of silver nanoparticles were characterized by the presence of a pronounced resonant band in the visible light region, called the surface plasmon resonance band, whose position depends on the size and shape of the nanoparticles [26]. Figure 1 shows the absorption spectrum of synthesized silver nanoparticles. The position of the main maximum at 400 nm with a width of less than 100 nm allowed us to conclude that the particles differ little in size and have an average diameter of 20 nm. The absence of additional absorption peaks indicated the dominance of spherical nanoparticles.

The obtained silver nanoparticles induced hemolysis of erythrocytes, the rate of which depended on the total concentration of silver and the ion content in the solution. Figure 2a presents the kinetics of erythrocyte hemolysis by nanoparticles at a silver concentration from 5 to 60 μM. As can be seen, the rate of hemolysis increased with an increase in the concentration of silver used for the synthesis of nanoparticles. At the same concentration of silver, hemolysis of erythrocytes with silver nitrate proceeded twice as fast as with nanoparticles (Fig. 2b).

Preliminary incubation of erythrocytes with hydrogen peroxide led to a decrease in the proportion of hemolysed cells destroyed by silver nanoparticles. The protective effect was manifested at a concentration of hydrogen peroxide in the range from 250 to 1500 μM.

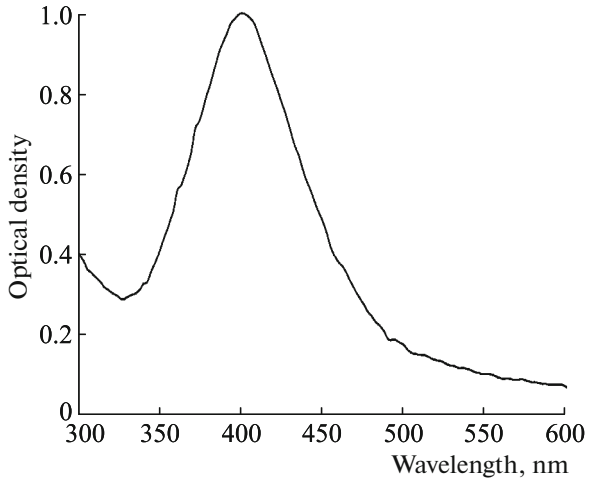

Fig. 1. Absorption spectrum of silver nanoparticles. The concentration of silver was 40 μM.

The proportion of non-hemolyzed cells increased to 0.8 (Fig. 3a). When erythrocytes were destroyed by silver nitrate, the protective effect of hydrogen peroxide was observed at lower concentrations, and the proportion of non-hemolysed cells reached 1 (Fig. 3b).

Based on the data on erythrocyte hemolysis, the values of the coefficients of destruction k_d and protection k_p at different concentrations of hydrogen peroxide were determined. The k_d coefficient characterized the toxic effect of silver ions and its value did not depend on the concentration of the oxidant, that is, it remained constant. The value of the k_p coefficient depended on the number of membrane complexes of methemoglobin, and, therefore, depended on the concentration of extracellular hydrogen peroxide, under the action of which the amount of methemoglobin and its membrane-bound form changed. The dependences of the protection coefficient on the concentration of hydrogen peroxide during destruction induced by silver nanoparticles and silver nitrate are shown in Fig. 4. As can be seen, the dependence of k_p on the concentration of hydrogen peroxide was a hormesis, that is, the value of the protection coefficient increased at low concentrations of the oxidant and decreased at high concentrations. Differences in the values of the cell protection coefficient under the action of different hemolytic factors were probably due to a change in the ratio of oxidized forms of hemoglobin and their membrane-bound forms over time.

The dependence of the binding kinetics of oxidized forms of hemoglobin with the membrane of human erythrocytes on intracellular and extracellular conditions was studied based on the proposed mathematical model. Within the model, it was assumed that extracellular hydrogen peroxide entered the cell by diffusion through the membrane, where it was utilized in reactions with hemoglobin and in reactions involving catalase and glutathione peroxidase. With an increase in the initial concentration of hydrogen peroxide, the rate of its diffusion and decomposition also increased. At concentrations below 1.5 mM and a cell count of 30 million cells, the breakdown time of extracellular hydrogen peroxide did not exceed 10 min. Thus, after the pre-incubation period (10 min), extracellular interaction between the oxidizer and nanoparticles was eliminated, and only the products of oxidation reactions remained in the cells.

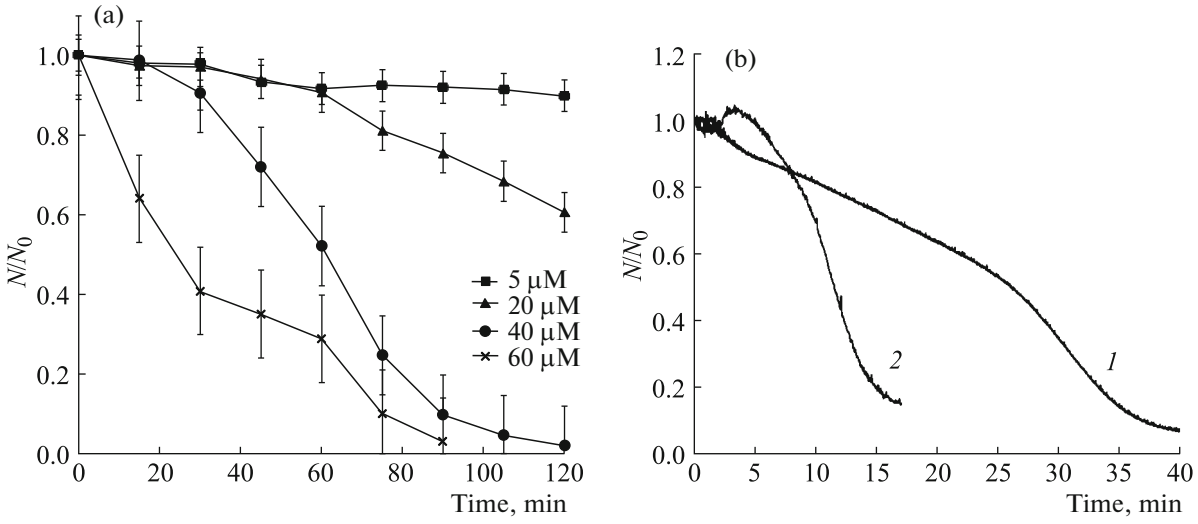

Fig. 2. (a) The kinetics of erythrocyte hemolysis induced by nanoparticles at different concentrations of silver; (b) the kinetic curves of erythrocyte hemolysis induced by nanoparticles (curve 1) and silver nitrate (curve 2) at a concentration of 100 μM. N/N_0 is the proportion of non-hemolysed erythrocytes, where N_0 is the initial number of erythrocytes in suspension, and N is the number of cells after hemolysis.

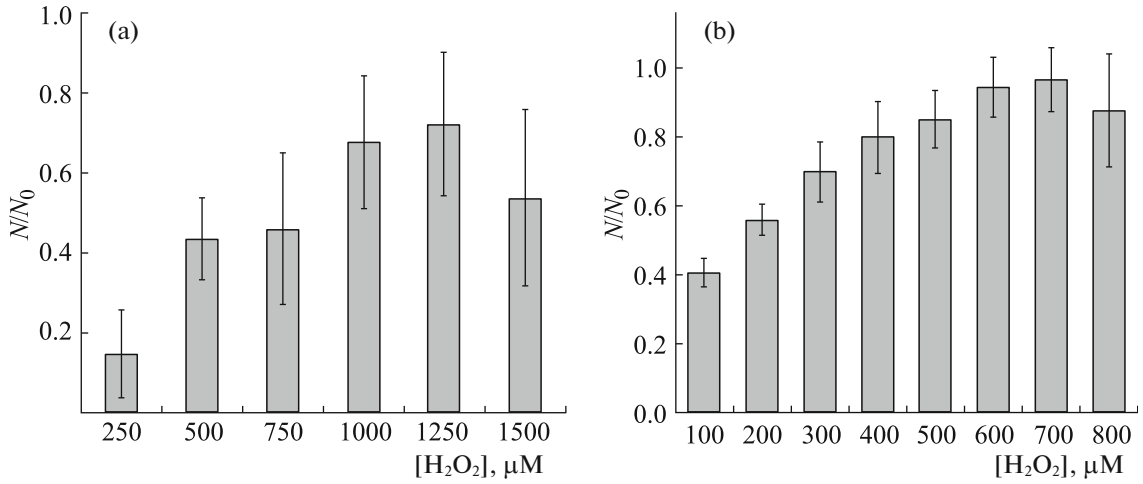

Fig. 3. The dependence of the proportion of non-hemolysed erythrocytes on the concentration of extracellular hydrogen peroxide during hemolysis induced by silver nanoparticles (a) and silver nitrate (b). N/N_0 is the proportion of non-hemolysed erythrocytes, where N_0 is the initial number of erythrocytes in suspension, and N is the number of cells after hemolysis.

Hemoglobin oxidation led to the formation of methemoglobin and ferryl hemoglobin, which reversibly bound to the components of the erythrocyte membrane. The number of membrane complexes of methemoglobin and ferryl hemoglobin depended on the number of corresponding proteins in the cytoplasm. The reduction of oxidized forms of hemoglobin was carried out by components of the antioxidant system of erythrocytes. With a decrease in the content of antioxidants, the recovery slowed down and the accumulation of oxidized forms of protein occurred. According to calculations, this effect occurred at concentrations of extracellular hydrogen peroxide above 300 μM. Figure 5 shows the absorption spectrum of hemoglobin complexes after osmotic destruction of erythrocytes incubated with hydrogen peroxide at a concentration of 250 μM. In the spectrum of hemolysate protein complexes of hydrogen peroxide-treated cells, a maximum shift from 415 to 405 nm was observed, which is a sign of the accumulation of methemoglobin, and not oxyhemoglobin on the membrane.

Within the proposed model of the adaptive mechanism, the degree of increase in the structural stability of the membrane was determined by the number of membrane–methemoglobin and membrane–ferryl hemoglobin complexes formed. The binding of met-

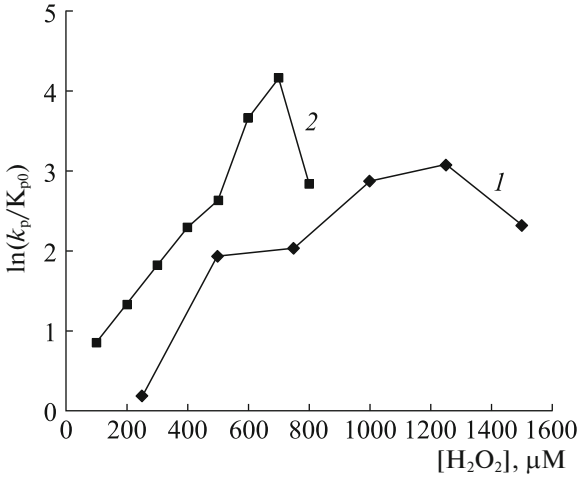

Fig. 4. The dependence of the protection coefficient on the concentration of hydrogen peroxide during hemolysis induced by silver nanoparticles (curve *1*) and silver nitrate (curve *2*); k_p is the protection coefficient under the action of hydrogen peroxide, and k_{p0} is the protection coefficient without hydrogen peroxide.

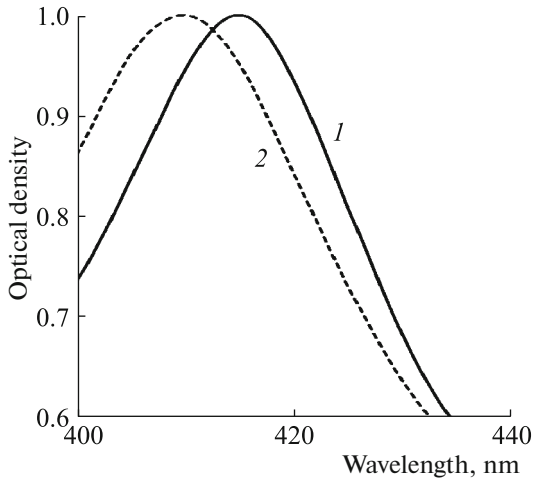

Fig. 5. The absorption spectrum of erythrocyte hemolysate in the control (curve *1*) and erythrocyte hemolysate incubated with hydrogen peroxide at a concentration of 250 μM (curve *2*).

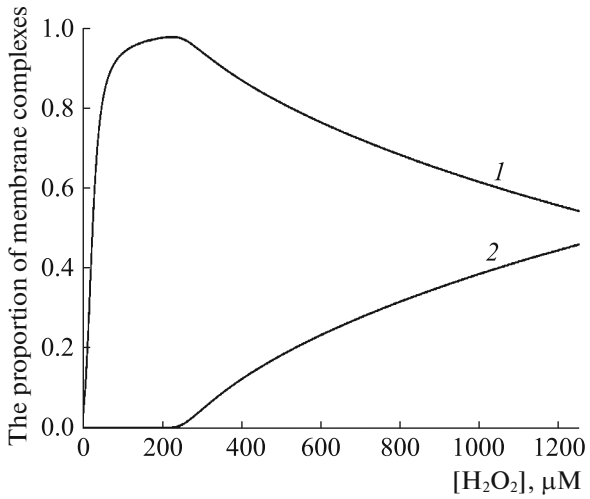

Fig. 6. The dependence of the proportion of membrane complexes of methemoglobin (curve *1*) and ferryl hemoglobin (curve *2*) on the concentration of extracellular hydrogen peroxide.

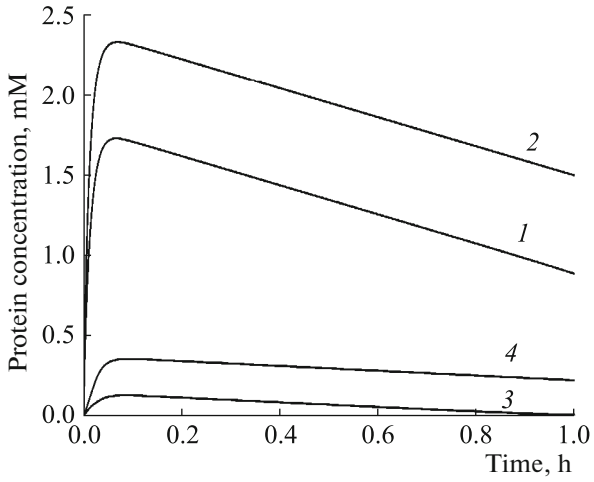

Fig. 7. The dependence of hydrogen peroxide-induced changes in the concentration of methemoglobin (curves *1* and *2*) and ferryl hemoglobin (curves *3* and *4*) on time. The concentration of hydrogen peroxide was 400 μM (curves *2* and *4*) and 600 μM (curves *1* and *3*).

hemoglobin to the membrane led to an increase in the structural stability of the membrane, while the formation of membrane—ferryl hemoglobin complexes, on the contrary, accelerated the processes of lipid peroxidation and disrupted the interaction of the cytoskeleton with the membrane. The amount of methemoglobin and ferryl hemoglobin complexes formed depended on the concentration of extracellular hydrogen peroxide, the incubation time, the number of cells in solution, the state of the erythrocyte antioxidant system, the metabolic activity of cells and the external metabolic conditions. Figure 6 shows the dependences of the number of membrane complexes of methemoglobin and ferryl hemoglobin on the concentration of extracellular hydrogen peroxide. As can be seen, at a low concentration of hydrogen peroxide in the cell, mainly methemoglobin membrane complexes were formed. A decrease in the pool of antioxidants in the cell and an increase in the concentration of hydrogen peroxide led to an increase in the proportion of ferryl hemoglobin membrane complexes.

Hydrogen peroxide at high concentrations led to a higher accumulation of oxidized forms of hemoglobin in the cell. The total amount of oxidized hemoglobin decreased over time due to enzymatic and non-enzymatic reduction. Figure 7 shows the results of numerical experiments on changes in the amount of methemoglobin and ferryl hemoglobin formed in cells at a concentration of hydrogen peroxide of 400 and 600 μM. It can be seen that the concentration of oxidized forms of hemoglobin decreased over time due to reduction. Thus, the increase in the protective properties of cells induced by hydrogen peroxide decrease with time.

Higher concentrations of hydrogen peroxide were needed for longer preservation of a high concentration of membrane complexes of methemoglobin. As a result, the position of the maximum of hormesis shifted towards high concentrations of the oxidant with an increase in the destruction time of erythrocytes after exposure to hydrogen peroxide. When erythrocytes were destroyed by silver nanoparticles, which took longer in comparison with hemolysis induced by silver nitrate, the maximum of the hormesis curve was observed at a concentration of hydrogen peroxide of 1250 μM (Fig. 3a); whereas the maximum of the hormesis curve in the case of silver nitrate was at 700 μM (Fig. 3b). The reduction of hemolysis time, on the contrary, led to a shift of the maximum of hormesis to lower concentrations of the oxidant. During osmotic hemolysis, when the destruction time was less than a minute, the protective effect reached a maximum at a concentration of hydrogen peroxide of 100 μM (Fig. 8).

It should be noted that the rate of damage to proteins under the action of silver nanoparticles and silver nitrate also differed. In the solution of oxyhemoglobin at the ratio of concentrations [Hb] : [$AgNO_3$] = 1 : 10, silver nitrate caused protein destruction and accumulation of aggregates within 1 h, which led to an increase in optical density at 600 nm in the absorption spectrum of the protein (Fig. 9a). Figure 9b shows the absorption spectrum of the oxyhemoglobin solution and its change upon the introduction of nanoparticles. As can be seen, less intensive interaction of silver nanoparticles with oxyhemoglobin led to the formation of aggregates in 3 h. Thus, higher concentrations of the oxidant were needed to preserve the protective properties of cells under slow damage to cells and pro-

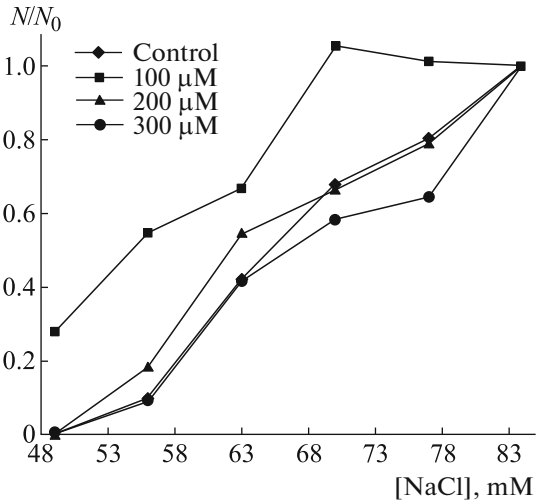

Fig. 8. The effect of hydrogen peroxide on the dependence of the proportion of non-hemolysed erythrocytes on the concentration of sodium chloride in solution. N/N_0 is the proportion of non–hemolysed erythrocytes, where N_0 is the initial number of erythrocytes in suspension, and N is the number of cells after hemolysis.

teins upon the action of silver nanoparticles compared with the action of silver nitrate.

CONCLUSIONS

The understanding of adaptation mechanisms at the molecular and cellular levels is a key stage in the creation of effective health-saving technologies. The mechanisms of regulation of adaptation of erythrocytes by hydrogen peroxide during hemolysis by silver nanoparticles were studied based on numerical modeling and spectrophotometric analysis.

Silver nanoparticles induced erythrocyte hemolysis the rate of which depended on the total concentration of silver and the ion content in the solution. Hemolysis of erythrocytes induced by silver nitrates proceeded twice as fast as that with nanoparticles.

Hydrogen peroxide reduced the proportion of hemolysed cells when erythrocytes were destroyed by silver nanoparticles and silver nitrate. Within the proposed model, the protection of cells under the action of hydrogen peroxide was due to the oxidation of hemoglobin, which led to the formation of a membrane-bound state of oxidized protein forms. Hemoglobin oxidation had a multidirectional effect on cell stability; namely, reversible binding of methemoglobin to the membrane led to an increase in the structural stability of the membrane. An increase in the concentration of ferrylhemoglobin and its binding to membrane components led to increased lipid peroxidation processes and impaired interaction of the cytoskeleton with the membrane.

The area of hormesis depended on the time of cell destruction under the action of a damaging factor. The maximum of the hormesis curve when damage was induced by silver nanoparticles was observed at a concentration of hydrogen peroxide of 1250 μM, and when damage was induced by silver nitrate it was at 700 μM. It was found based on numerical modeling, that the dependence of the maximum of the hormesis curve on the concentration of extracellular hydrogen peroxide and incubation time was due to the dynamic nature of the cytoplasmic mechanisms regulating the ratio of membrane complexes of methemoglobins and ferrylhemoglobins. Thus, the dynamics of the binding of methemoglobin and ferrylhemoglobin to the membrane played a key role in their ability to protect erythrocytes from destruction induced by silver nanoparticles and other damaging factors.

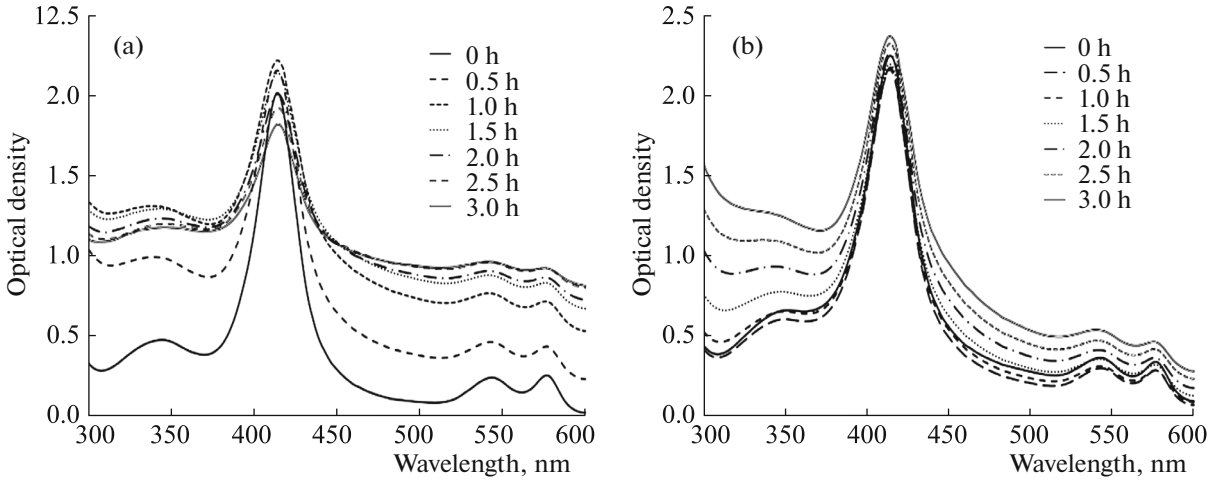

Fig. 9. Changes in the absorption spectrum of the oxyhemoglobin solution over time upon introduction of silver nitrate (a) and silver nanoparticles (b).

FUNDING

The work was partially supported by the Belarusian Republican Foundation for Basic Research, project no. B22-045.

CONFLICT OF INTEREST

The authors declare that there is no conflict of interest.

COMPLIANCE WITH ETHICAL STANDARDS

This article does not contain a description of studies involving humans and animals as objects.

REFERENCES

1. C. Lopez-Otin and G. Kroemer, Cell **184** (1), 33–63 (2021).
2. G. G. Martinovich, *Reactive Oxygen Species in the Regulation of Functions and Properties of Cells: Phenomena and Mechanisms* (BGU, Minsk, 2021) [in Russian].
3. H. Sies and D. P. Jones, Nat. Rev. Mol. Cell Biol. **21** (3), 1 (2020).
4. N. K. Zenkov, A. V. Chechushkov, P. M. Kozhin, et al., Biochemistry (Moscow). **82** (5), 556 (2017).
5. G. G. Martinovich, I. V. Martinovich, A. V. Vcherashnyaya, et al., Biophysics **65** (6), 942 (2020).
6. A. V. Ulasov, A. A. Rosenkranz, G. P. Georgiev, et al., Life Sci. **291**, 120111 (2021).
7. O. V. Kosmachevskaya, E. I. Nasybullina, V. N. Blindar, et al., Applied Biochem. Microbiol. **55** (2), 83 (2019).
8. N. Arashiki, N. Kimata, S. Manno, et al., Biochemistry **52**, 5760 (2013).
9. E. M. Welbourn, M. T. Wilson, A. Yusof, et al., Free Radical Biol. Med. **103**, 95 (2017).
10. L. M. Snyder, N. L. Fortier, J. Trainor, et al., J. Clin. Invest. **76**, 1971 (1985).
11. S. A. Mendanha, J. L. V. Anjos, A. H. M. Silva, et al., Braz. J. Med. Biol. Res. **45**, 473 (2012).
12. A. Kinoshita, Y. Nakayama, T. Kitayama, et al., FEBS J. **274**, 1449 (2007).
13. P. Jarolim, M. Lahav, S. C. Liu, et al., Blood **76**, 2125 (1990).
14. V. V. Voinarovskii and G. G. Martinovich, Biochem. (Moscow) Suppl. Ser. A. **39** (1), 91 (2022).
15. O. Gherasim, R. A. Puiu, A. C. Birca, et al., Nanomaterials **10** (11), 2318 (2020).
16. C. Liao, Y. Li, and S. C. Tjong, Int. J. Mol. Sci. **20**, 449 (2019).
17. I. X. Yin, J. Zhang, I. S. Zhao, et al., Int. J. Nanomed. **15**, 2555 (2020).
18. D. He, A. M. Jones, S. Garg, et al., J. Phys. Chem. C **115**, 5461 (2011).
19. H. Holzhutter, Eur. J. Biochem. **271**, 2905 (2004).
20. G. G. Martinovich and S. N. Cherenkevich, Biomed. Khim. **51** (6), 626 (2005).
21. R. M. Johnson, G. Jr. Goyette, Y. Ravindranath, et al., Free Radical Biol. Med. **39**, 1407 (2005).
22. F. Orrico, M. N. Moller, A. Cassina, et al., Free Radical Biol. Med. **121**, 231 (2018).
23. L. Gebicka and E. Banasiak, Acta Biochim. Pol. **56** (3), 509 (2009).
24. A. Kinoshita, Y. Nakayama, T. Kitayama, et al., FEBS J. **274**, 1449 (2007).
25. X. D. Peng, M. P. Washburn, G. P. Sun et al., Biochem. Biophys. Res. Comm. **221** (1), 117 (1996).
26. Yu. A. Krutyakov, A. A. Kudrinskii, A. Yu. Olenin, et al., Usp. Khim. **77** (3), 242 (2008).

Translated by E. Puchkov